JOURNAL OF PROPULSION AND POWER
Vol. 20, No. 6, November–December 2004

Characterization of Cathode Keeper Wear by Surface Layer Activation

Robert D. Kolasinski*
California Institute of Technology, Pasadena, California 91125
and
James E. Polk†
Jet Propulsion Laboratory, California Institute of Technology, Pasadena, California 91109

The erosion rates of the discharge cathode keeper in a 30 cm NASA Solar Electric Propulsion Technology Applications Readiness (NSTAR) configuration ion thruster were measured using a technique known as surface layer activation (SLA). This diagnostic involved producing a radioactive tracer in the keeper surface by high-energy proton bombardment. The decrease in activity of the tracer material was monitored with a gamma spectroscopy system after the surface was subjected to wear processes. Correlation with a depth calibration curve yielded the eroded depth. The primary objectives were to validate the technique by reproducing erosion data from previous wear studies and to determine the effect of different engine operating parameters on erosion rate. The erosion profile at the TH 15 (2.3-kW) setting observed during the 8200-h life demonstration test was reproduced with a measured maximum erosion rate of 0.085 μm/h. Testing at the TH 8 (1.4-kW) setting demonstrated that variations in keeper voltage had a significant effect on the erosion, with a positive bias with respect to cathode potential decreasing the wear rate significantly. Measurements were achieved after operating times of 40–90 h, with a typical uncertainty of $\pm$0.003 μm/h.

Nomenclature

a	=	reference count rate, cps
h	=	number of isotopes present in sample spectrum
m	=	spectrum scaling parameter
$\dot{m}$	=	mass flow rate, standard cm^3
n	=	total number of channels in sample spectrum
P_{tot}	=	total thruster power, kW
T	=	thrust, mN
W	=	weight factor array
y	=	sample count rate, cps
z	=	total counts
η_{tot}	=	total thruster efficiency
τ	=	spectrum live time, s

Subscripts

A	=	accelerator grid
B	=	beam
CK	=	cathode keeper
D	=	discharge
i	=	channel
j	=	isotope
NK	=	neutralizer keeper

Superscripts

b	=	background spectrum
r	=	reference spectrum
s	=	sample spectrum

Introduction

ION engines have been used for a variety of applications, such as NASA deep space propulsion, station keeping, and orbit raising. There has been a large increase in interest in the use of ion thrusters as the primary propulsion system for robotic interplanetary spaceflight due to the success of the xenon ion thruster on NASA's Deep Space 1 (DS1) technology demonstration mission, launched on 24 October 1998. The thruster itself was developed as part of the NASA Solar Electric Propulsion Technology Application Readiness (NSTAR) program and features a ring-cusp discharge chamber design, 30-cm-diam ion optics, and a 6.35-mm-diam hollow cathode. At its maximum throttle setting, which corresponds to an input power of 2.3 kW, the ion engine operates with an I_{sp} of approximately 3100 s and is capable of producing a thrust of 92 mN. These performance parameters make this type of thruster ideal for missions to the inner planets and asteroid belt. Higher power ion engine designs are currently being pursued for applications such as outer planet orbiters and sample return missions, which will require ΔV in excess of 40 km/s (Ref. 1). Because the burn time required for many of these missions is on the order of 5–10 years, being able to accurately predict the service life of these thrusters is of great importance.

Evaluating the lifetime of discharge cathodes has been of great interest throughout the history of ion engine design because their failure modes are generally considered to be among the major life-limiting mechanisms of these thrusters.[2] Wear processes specifically associated with the discharge cathode assembly include failure of the heater, cathode orifice plate, and keeper electrode due to sputter erosion. During a 2000-h wear test of an NSTAR engineering model thruster (EMT1), significant erosion of the hollow cathode was observed.[3] An engineering solution to this problem was to include an enclosed keeper electrode into the design. This was found almost to eliminate cathode orifice plate erosion during a subsequent 1000-h wear test.[4] Significant wear of the keeper can leave the hollow cathode vulnerable to ion bombardment, however, eventually leading to failure of the cathode orifice plate and heater. These wear

Presented as Paper 2003-5144 at the AIAA/ASME/SAE/ASEE 39th Joint Propulsion Conference and Exhibit, Huntsville, AL, 20–23 July 2003; received 1 November 2003; revision received 20 April 2004; accepted for publication 20 April 2004.

*Graduate Student, Department of Mechanical Engineering, Division of Engineering and Applied Science, Mail Code 301-46; rdk@caltech.edu. Student Member AIAA.

†Principal Engineer, Thermal and Propulsion Engineering, Mail Code 125-109. Member AIAA.

phenomena are not currently understood well enough to predict cathode service life accurately.

In this investigation, a diagnostic technique known as surface layer activation (SLA) is used to measure the erosion of the discharge cathode keeper in an NSTAR configuration ion thruster. The keeper erosion observed in life tests is reviewed, along with an overview of the SLA process. A discussion of the experimental method and associated errors is provided. The results of a series of keeper wear tests are presented for a variety of different operating conditions.

Summary of Discharge Cathode Keeper Erosion Data

Recent long-duration wear tests revealed that the cathode keeper is especially susceptible to rapid wear. Results from these tests served as a baseline for comparison with the experiments conducted in this study. An 8200-h life demonstration test (LDT) of an NSTAR engineering model thruster (EMT2) was conducted before the launch of DS1. The set points for a number of NSTAR throttle levels are shown in Table 1. The thruster was operated at the TH 15 (2.3-kW) throttle setting for the duration of the LDT, the maximum power level for this ion engine. Destructive analysis after the conclusion of the test revealed that approximately 30% of the orifice plate of the keeper had worn away during operation. In addition, significant chamfering near the orifice had also occurred.[5] Figure 1 shows this erosion profile, along with the original geometry

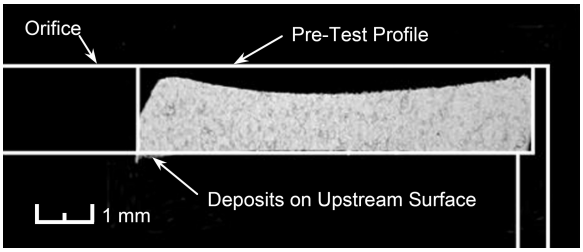

Fig. 1 Cross section of the cathode keeper orifice plate from the 8200-h LDT showing the erosion profile.[5]

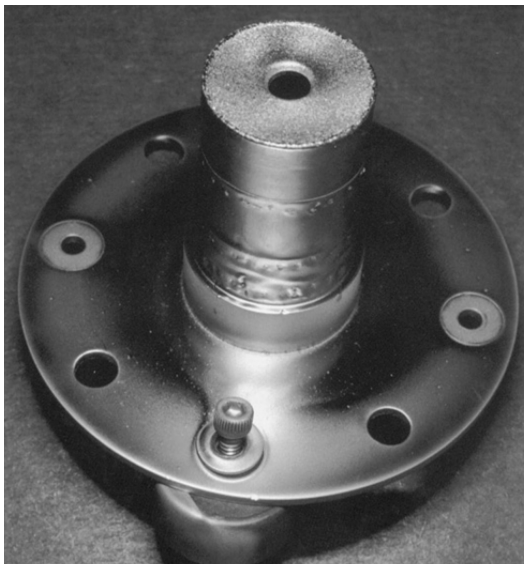

Fig. 2 EMT2 keeper after 8200 h operation.

of the orifice plate. The maximum erosion rate over the duration of the test was approximately 0.063 μm/h. The downstream surface of the cathode keeper, as it appeared at the end of the LDT, is shown in Fig. 2. After a 1000-h test conducted under the same operating conditions just before the LDT, profilometry of the keeper revealed a similar wear pattern with a maximum erosion rate of approximately 0.070 μm/h (Ref. 6). In addition, recent laser-induced fluorescence (LIF) measurements of sputtered Mo density just downstream of the keeper indicated peak densities that correlate well with the regions of maximum erosion on the keeper surface suggested by Fig. 1.[7]

After the completion of the LDT, an extended life test (ELT) of the DS1 flight spare ion thruster (FT2) was conducted at the Jet Propulsion Laboratory (JPL). This test represents the longest wear test of an ion engine to date, having accumulated 30,352 h of operation at a number of different operating conditions. The ELT vacuum facility was equipped with a diagnostics platform, which included a camera capable of photographing the keeper through the grids of the thruster. The first 4937 h of the test were conducted at higher power levels (TH 12 and TH 15), and the keeper wear pattern appeared to mimic that observed in the 1000- and 8200-h tests. When the engine was throttled down to TH 8, the erosion profile appeared to change significantly, with increased wear near the orifice. The orifice rapidly widened over the next 5000 h at TH 8, a process which continued even after operation at TH 15 resumed. It was suspected that the change in throttle level coupled with an intermittent short between the keeper and the cathode over a 3023-h period contributed significantly to the increased wear. At the conclusion of the test, the keeper orifice plate had been almost completely destroyed.[8]

SLA

SLA is a sensitive diagnostic, which can be used to measure rapidly keeper wear under a variety of thruster operating conditions. The general technique involves bombarding the material under consideration with a high-energy ion beam produced by a particle accelerator or cyclotron. The ions colliding with the surface have a known probability of causing a nuclear reaction, which transmutes some of the target atoms to a radioactive isotope. Knowledge of the beam energy, angle of incidence, and reaction cross sections allows the activity per unit depth to be calculated. The depth calibration is also determined directly by activating a stack of uniform foils and measuring their relative activities. Before the actual experiment is to be conducted, the activity level of the tracer material is recorded via a gamma spectroscopy system. After the test has concluded, another spectrum is recorded, and a scaling parameter between the two spectra is determined and correlated with a total mass loss.

Because of the high sensitivity of SLA, it was expected that accurate measurements could be obtained after 40 h of thruster operation based on the erosion rates seen in previous life tests. The technique allows localized measurements to be made because only the material in the activated region is monitored. In general, the width of the activated region is limited by the beam diameter and the masking techniques used, which in this case allowed for activated bands approximately 1 mm wide. One of the most attractive attributes of this technique is that the decrease in activity represents a direct measure of mass loss. The relationship between the measured signal and the erosion rates is governed by a simple depth calibration curve that is known accurately. There is no need to infer erosion rates from the densities or emission spectra of sputtered particles, as is the case with many other techniques.

Table 1 DS1 ion thruster throttle points

TH level	P_{tot}, kW	$\dot{m}_{\text{cath}}$, standard cm^3	$\dot{m}_{\text{neut}}$, standard cm^3	$\dot{m}_{\text{main}}$, standard cm^3	V_B, V	J_B, A	V_A, V	J_{NK}, A
0	0.52	2.47	2.40	5.98	650	0.51	−150	2.0
3	0.85	2.47	2.40	6.85	1100	0.61	−150	2.0
6	1.21	2.47	2.40	11.33	1100	0.91	−150	2.0
8	1.46	2.47	2.40	14.41	1100	1.10	−180	1.5
12	1.96	2.89	2.81	19.86	1100	1.49	−180	1.5
15	2.33	3.70	3.60	23.42	1100	1.76	−180	1.5

SLA has been used frequently in the automotive industry as a method of measuring wear rates of components in internal combustion engines.[9] In this case, a $Fe^{56}(p,n)Co^{56}$ reaction is utilized, and the wear rate is measured in real time by monitoring the radioactivity of the engine oil. It has also been applied to measuring the wear of railway rails and cutting tools, the effectiveness of different lubricants, and in corrosion studies.[10] In materials that can not be directly activated, such as plastics and carbon composites, recoil implantation may be used.[10,11] In electric propulsion applications, SLA has been applied at Princeton University in magnetoplasmadynamic (MPD) thruster cathode erosion studies.[12,13]

Activation Parameters

The activation parameters depend on the target material, the desired reaction products, and the required sensitivity. Reactions that result in tracer materials with half lives of several months are ideal for SLA applications because the decay rate is sufficiently fast to minimize facility contamination hazards, while allowing for a reasonably long testing window. In addition, it is desirable to have only a single reaction product because multiple overlapping photo-peaks require higher resolution equipment and more complex data analysis procedures. The software used to analyze the spectra in this study is capable of resolving multiple components, although to do so, a reference spectrum for each would be required. To increase the sensitivity, the proton beam may be angled with the target surface, thereby compressing the activated region into a thinner layer. This has the effect of increasing the amount of activity per unit depth, providing higher resolution.

The cathode keepers used in this investigation were fabricated to the same specifications used for the NSTAR flight thrusters. The keeper itself consists of a 19.0-mm- (0.75-in.-) diam tantalum tube with a 1.5-mm- (0.06-in.-) thick molybdenum orifice plate electron beam welded to the downstream end. The orifice hole diameter is 4.8 mm (0.1875 in.). To eliminate any differences in the activation profiles due to surface roughness, the downstream surface of each orifice plate was polished to a 1-μm finish. The keepers were activated by bombarding the molybdenum orifice plate with a 10.4-MeV proton beam. This resulted in two nuclear reactions, which transmuted a small percentage of the Mo^{95} to the gamma-emitting technetium isotopes, Tc^{95m} and Tc^{96}:

$$Mo^{95}(p, n)Tc^{95m}, \qquad Mo^{95}(p, n)Tc^{96}$$

The reaction yield for Tc^{96} is actually 60 times higher than that of Tc^{95m} (Ref. 10). However, because its half-life is so short, its activity drops to negligible levels after approximately two months, allowing the spectrum to be analyzed as though it was produced by one isotope only. High-resolution Ge(Li) detector scans confirmed that the Tc^{96} contributed only minimally to the total activity measured.

Three keepers were activated, each at a different radial location based on the erosion profile which resulted from the 8200-h test. The activated sites were circular bands concentric with the orifice, each 1 mm wide. Activating in thin bands rather than small spots (as is typically done in many industrial applications) decreased the dosage per unit area of the part, thereby decreasing the potential for radiation damage to the surface. Furthermore, this type of activation mitigated the effects of any asymmetries in the erosion pattern. A radiograph of the activated regions of the keepers using gamma sensitive paper is shown in Fig. 3. The gaps in the activated areas are due to the masking technique used during the activation process. The total activity of each band was 2 μCi, 50% of which was within 30 μm of the surface. The shallow depth was achieved by angling the proton beam 60 deg with respect to the orifice plate surface. The keeper with the smallest diameter activated ring was subjected to the most severe dose from the proton beam, at a level of 0.040 $\mu A \cdot h/mm^2$ (1.4×10^{-4} C/mm^2). For these conditions, the ratio of number density of Tc^{95m} to Mo^{95} was calculated to be on the order of 10^{-26}.

Calculation of the Depth Calibration Curve

The depth calibration used in this study is derived from both previous experimental measurements and calculations based on reaction cross section data. The experimental method involves activating a stack of foils of uniform thickness (on the order of several micrometers). The activity in each foil may then be measured in relative amounts by gamma spectroscopy. The calculated profile was produced with a software package known as TLAPrfl.[14] The software utilizes existing foil stack data at known beam energies for 63 different reactions. Empirical relationships and stopping power data from Ziegler[15] are used to extrapolate to intermediate activation energies.

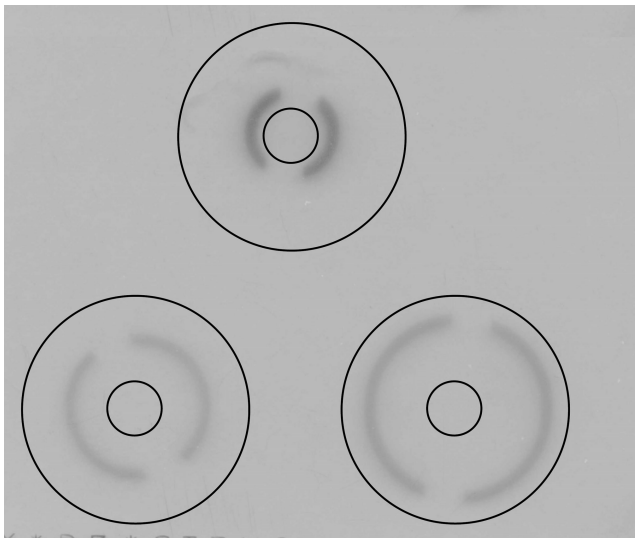

Fig. 3 Radiograph of activated cathode keepers obtained with gamma-sensitive photographic paper. Black outlines indicate the keeper orifice geometry (courtesy Kenneth Oxorn, ANS Technologies).

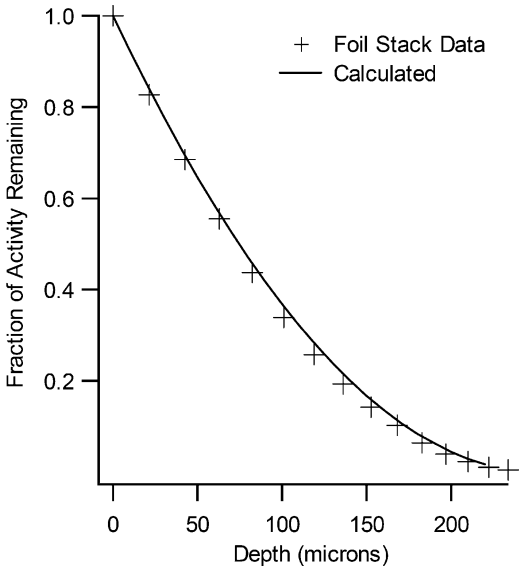

Fig. 4 Activity vs depth profile for 11-MeV proton beam activation of Mo^{95}.

Figure 4 shows a depth calibration curve for an 11-MeV activation of Mo^{95} at normal incidence. The experimental data obtained from Ref. 10 is shown with the calculated profile for this case. The agreement between the two curves is excellent, especially for depths less than 50 μm. A detailed analysis of the errors associated with these curves appears in a subsequent section.

Experimental Procedure

The SLA experiments were designed to minimize the turn-around time between subsequent runs and to make the conditions of each test as repeatable as possible. Before each test, a reference spectrum of an activated keeper was collected over a 12-h period. Once this was completed, the keeper was mounted to a cathode and installed in a laboratory mock-up of the DS1 flight thruster. The thruster

itself remained mounted in the vacuum chamber inasmuch as it was designed to allow the cathode to be extracted easily from the back magnet ring by simply removing a portion of the plasma screen and disconnecting the propellant line and electrical leads. After the engine was reassembled, the chamber was pumped down, and the cathodes were conditioned according to the same procedures used during the ELT. Once the thruster was started, typically 20–30 min were required for its operating parameters to stabilize, after which an automated data acquisition system controlled and monitored the test conditions. After the completion of each experiment, the vacuum system was vented up to atmospheric pressure, and the described process was repeated for each subsequent experiment. A typical test required approximately 1 week to complete.

Between tests, the cathodes were stored in a nitrogen purge box to prevent contamination. Once the eroded keeper was removed from the thruster, another gamma spectrum was collected and compared to the pretest reference data. Special care was taken to minimize handling keepers to not damage or contaminate them during this process. The only material that came into contact with the downstream surface of the keeper was a Teflon® sleeve used to ensure repeatable positioning of the keeper within the detector and to prevent contamination of the detector itself. A background scan with only the sleeve in the detector was taken after each spectrum was collected to ensure that none of the radioactive material had been removed from the downstream surface.

The gamma spectroscopy system that was used to measure the activity of the samples included a NaI(Tl) scintillation detector containing a 7.6 by 7.6 cm cylindrical crystal. The samples were loaded in a 5.1-cm-deep, 2.5-cm-diam cavity in the detector. The crystal emits a number of photons proportional to the energy of the incident gamma that it absorbs. The base of the crystal is attached to a photomultiplier tube (PMT) that generates a voltage signal based on the number of photons emitted by the crystal. The entire assembly is encased in a copper-lined lead shield to filter out background radiation. The voltage signal is processed by a multi-channel analyzer.

To obtain high resolution scans, a Ge(Li) semiconductor detector available at the California Institute of Technology was used. The higher resolution was necessary to detect impurities in the activated samples because the photopeaks from the contaminant isotopes were rather close to those of Tc^{95m}. Only one line from Tc^{96} could be discerned, at 849.9 keV.

A comparison of the spectra obtained with each type of detector is shown in Fig. 5. Prominent photopeaks and half-life data are shown in Table 2.

Although the Ge(Li) detectors offer much better energy resolution, NaI(Tl) detectors were favored in this study. Because the spectrum is essentially composed of only one isotope, and all of the photopeaks decay at the same rate, there was no significant penalty for using these types of detectors. Furthermore, the counting efficiency of the NaI(Tl) detectors is superior to the semiconductor

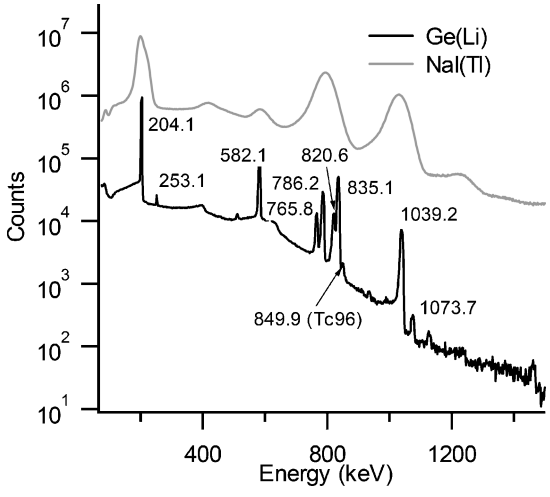

Fig. 5 Tc^{95m} spectra scans from Ge(Li) and NaI(Tl) detectors.

Table 2 Properties of activated products over the range of interest of this experiment

Isotope	Photopeaks, keV	Half life, days
Tc^{95m}	204.1, 582.1, 1039.2	58.72 ± 0.15
Tc^{96}	778.2, 812.5, 849.9	4.28 ± 0.07

detectors. Hence, shorter counting times are required, enabling a faster turn-around time between tests.

Data Analysis

The method of resolving the scaling parameter between the gamma spectra is an iterative least-squares scheme. This method has been successfully employed in the past at Oak Ridge National Laboratories to determine the concentrations of radioactive contaminants in chemical solutions.[16] The method was later enhanced to allow for the measurement of MPD thruster wear rates.[13]

The sample count rate in a particular channel i is given by

$$y_i = \left(z_i^s / \tau^s\right) - \left(z_i^b / \tau^b\right)$$

The sample spectrum may be the composite of several reference spectra. The count rate in the reference spectrum for a particular channel i produced by an isotope j is given by

$$a_{ij} = \left(z_{ij}^r / \tau_j^r\right) - \left(z_{ij}^b / \tau_j^b\right)$$

The relationship between the two spectra is

$$y_i = \sum_{j=1}^{h} a_{ij} m_j + \varepsilon_i$$

The objective of the weighted least-squares method is to find a solution $\hat{m}_j$ that minimizes the error term ε_i according to some weight factor matrix W_{ij}. The diagonal elements of $\boldsymbol{W}$ are generally the inverse of the count rates in each of the channels, to mitigate the effect of peak broadening in the experimental data. As a result, the best fit provided by the least-squares method is given by

$$\hat{\boldsymbol{m}} = (\boldsymbol{a}^T \boldsymbol{W} \boldsymbol{a})^{-1} \boldsymbol{a}^T \boldsymbol{W} \boldsymbol{y}$$

Large errors may occur if there is significant gain and threshold drift in the instrument electronics. The least-squares methodology is ideally suited to correcting for such errors. Details of the implementation of these methods may be found in either Ref. 13 or 16.

Error Analysis

The greatest advantage in using SLA to measure low wear rates is the high accuracy that is attainable. To ensure this level of accuracy is achieved, a careful examination of sources of error was conducted.

Error in the scaling parameter between the sample and reference spectrum arises from statistical fluctuations in the count rate of each channel. This uncertainty is given by[13,16]

$$\hat{\sigma}^2(\hat{m}_j) = \frac{1}{n-h}\left(\sum_{i=1}^{n} W_{ii} a_{ij} a_{ij}\right)^{-1} \sum_{i=1}^{n} W_{ii}\left(y_i - \sum_{j=1}^{h} a_{ij}\hat{m}_j\right)^2$$

Note that, for a given channel, the statistical fluctuation is approximated by

$$\sigma^2(y_i) = \left[\left(y_i^s + y_i^b\right)/\tau^s\right] + \left(y_i^b/\tau^b\right)$$

From this relationship, it is clear that the two steps that may be taken effectively to reduce the variance in count rates are reducing the background count rate by surrounding the detection system with lead shielding and increasing the collection live times. In this study, collection times in excess of 10^4 s were used, making statistical noise an insignificant source of error in the measurements.

The PMT of the detection system also introduces a potentially significant error source. The PMT heats up during operation, causing amplifier gain and threshold shifting. To eliminate this effect, a software gain stabilization is implemented as the spectrum is being collected. The gain is actively controlled to maintain a single photopeak in a specified energy window. This is sufficient to eliminate almost all threshold shifting and to hold the gain shifting to within 3%. A secondary software correction is used after the spectra are collected to eliminate the gain shifting completely. Tests of the gain and threshold shift correction methods demonstrated that this source of uncertainty does not contribute significantly to the measurement error.

The measured reduction in activity must be corrected for the natural decay of the radioisotope. This introduces another factor affecting the measurement precision, namely, the uncertainty in the half-life of Tc^{95m}. The published value is 61 ± 2 days, from a 1959 study by Unik and Rasmussen.[17] This value was arrived at by a technique known as peak stripping, which is less accurate than the least-squares fitting scheme employed in this study. The half-life of a pure Tc^{95m} sample was measured as part of this study, yielding a value of 58.72 ± 0.15 days. The improved measurement is due primarily to enhancements in the analysis method (iterative least squares) and that technetium can be more readily produced in a purer form today than when the previous study was undertaken. The half-life measurement was also used as a test for the data analysis software before running the actual wear experiments.

In addition, the trace amounts of Tc^{96} remaining in the activated samples during the early portion of the testing affected the count rates. Typically, the Tc^{96} contribution to the spectrum was less than 0.33% of the total number of counts. Furthermore, the short half-life of this isotope (4.2 days) made it significant only in the first two tests conducted. The error due to the decay of these contaminants is a slight overprediction of the wear rate.

The depth calibration curve was expected to be the largest source of error in the SLA measurements. Error associated with this curve arises from uncertainty in both the published experimental data at different energies and how well the calculated calibration fits these data for intermediate energies. In the foil stack data, foil thicknesses are measured via a precision microbalance. The relative activity present on each foil is measured via a gamma spectroscopy system similar to that used in this study. The uncertainty in the foil thickness can be converted to an error in activity level, allowing it to be added to the statistical error in the activity measurement. The depth calibration curve is nearly linear for shallow depths (less than 15 μm). To determine how well the interpolated curve over this shallow range agreed with measured data, experimental measurements from an 11-MeV activation were compared to the calculated profile. Calculations of linear fits over the range of interest indicated a worst-case error in slope of $\pm 3.5\%$ due to uncertainty in the agreement between the foil stack data and the calculated depth profile.

There are also uncertainties introduced by the wear process itself. If the eroded depth is uneven across the activated region, the perceived depth may be skewed depending on the shape of the depth calibration curve in this region and the degree to which the erosion is nonuniform. This problem is avoided by having a uniform density distribution within the activated region, which is essentially true over the range of interest considered here.

Radiation damage is another factor that may affect the sputtering characteristics of the activated samples, although the amount that is considered to be significant is often subjective. One measure of radiation damage is the number of displacements per atom (dpa). This may be interpreted as the number of times an atom undergoes a displacement from its lattice position during a collision cascade. For proton activations of metallic materials, the primary mechanism by which incident particles lose energy is through interactions with the electrons in the target. For this type of interaction, the Rutherford cross section is appropriate, an approximation of which was calculated and used in this analysis. Electronic interactions dominate through most of the range of interest, and most nuclear interactions occur below 120 μm. Using the methodology presented in Ref. 18, a dpa of 5×10^{-5} was calculated for the activations in this study, suggesting that the effects of radiation damage would be minimal.

Redeposition of sputtered material on the keeper surface is another concern because such material would be indistinguishable to the detector from the activated bands and would cause an underestimation of total wear. The fact that there is no direct line of sight from the keeper to itself makes it unlikely that sputtered products would be redeposited. To determine where most of the material was deposited experimentally, a series of witness plates were attached to different locations on the interior of the thruster discharge chamber during one of the experiments. Measurements of the activity of the material coating the plates after testing confirmed that most of the sputtered products from the keeper were deposited on surfaces near the grids. The activity accumulated on witness plates mounted near the cathode region was on the order of 10^{-6} times less than the total activity of the keeper itself, suggesting that error due to deposition in this region is negligible.

Erosion Experiments

Thruster Hardware

A laboratory model of the NSTAR thruster (known as the NKO thruster) was developed for use in this investigation because contamination concerns precluded using any of the EMTs. The NKO discharge chamber is of aluminum construction, with the magnets themselves and their placement identical to those used on the flight engines. In addition, the orifice geometry of the 0.635-cm- (0.25-in.-) diam laboratory model cathode was identical to those of FT2 and EMT2.

Detailed magnetic field maps of the cathode region of NKO and FT2 indicated that the field strength was accurately replicated, with the axial field strength at the cathode tip within 3.5% in NKO. The thruster was outfitted with a molybdenum grid set from a J-series thruster. The grids were fabricated with the same hole geometry as the later NSTAR series thrusters. The grids in this study had been used in previous tests, and the hole diameter had enlarged to a maximum of 1.2 mm, which falls between the original 1.14-mm and the 1.4-mm hole size observed at the end of the 8200-h test. The gap between the ion optics assembly and the downstream magnet ring was adjusted so that it was identical to that of FT2.

All testing was conducted in JPL's 2.5×5.5 m Thruster Performance and Endurance Test Facility. The chamber itself is equipped with three cryogenic pumps, producing a base pressure of 1.1×10^{-5} Pa (8.0×10^{-8} torr). During thruster operation, the maximum pressure was 2.7×10^{-3} Pa (2.0×10^{-5} torr). All pressures were measured with an ion gauge calibrated for N_2. The tank pressure is divided by a gas correction factor of 2.874 to obtain the ambient pressure in xenon. The discharge chamber propellant flow rate was corrected for ingestion of ambient gas, assuming free molecular flow using the measured chamber pressure. The chamber is equipped with an E × B probe and two Faraday probes. The power supply system was composed of components similar to those used on the recently completed ELT.[8] A data acquisition system also similar to that used during the ELT allowed for measurement of the thruster electrical parameters to within $\pm 0.5\%$.

A preliminary test was conducted to verify that the thruster performed similarly to the DS1 ion thruster over the entire NSTAR throttle range. In general, the agreement between the NKO and FT2 values before life testing was excellent, as demonstrated in Table 3. Furthermore, the measured double ion fraction and keeper ion current also matched closely with those measured during an earlier series of tests with EMT4, as shown in Table 4.

The NKO thruster's discharge parameters also fall well within the spread of values observed from wear testing of EMT2 and FT2, as well as performance testing of EMT4. This provides confidence that the NKO thruster accurately reproduces the discharge chamber environment of NSTAR thrusters. This is shown in Fig. 6, where the discharge parameters for these thrusters are compared with those of the NKO. The average value of each operating parameter is indicated by the triangular marker, and the extent of the maximum and minimum values obtained during long duration testing is indicated by bands when applicable.

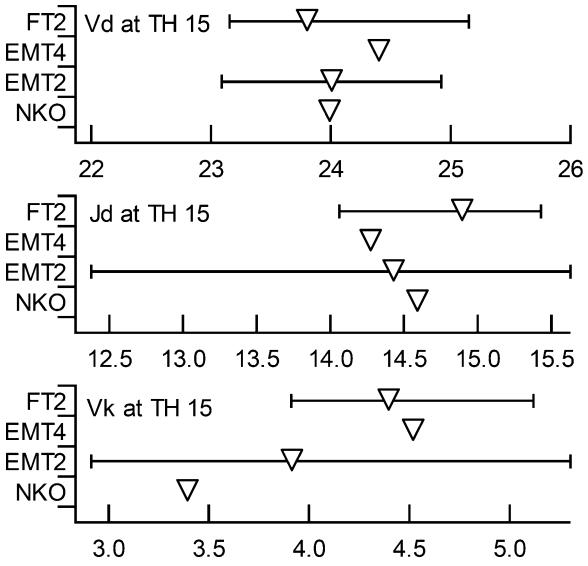

Fig. 6 Range of discharge parameters for NSTAR configuration thrusters.

Table 3 NKO vs FT2[a] performance data over the entire NSTAR throttle range

	NKO		FT2	
TH level	J_D, A	V_D, V	J_D, A	V_D, V
0	5.06	25.45	4.64	25.97
3	5.73	26.35	5.37	27.06
6	8.10	25.00	7.42	25.37
8[b]	9.18	24.90		
12	11.70	25.19	10.83	25.17
15	14.60	24.00	14.06	24.45

[a]FT2 performance data taken as part of a performance acceptance test before starting the ELT.
[b]Performance acceptance test data not available at TH 8 for FT2 pretest conditions.

Table 4 NKO vs EMT4 keeper ion current and double ion current along thruster centerline

	Keeper ion saturation current, mA		$J++/J+$	
TH level	NKO	EMT4	NKO	EMT4
8	127	121	0.273	0.225
15	191	187	0.303	0.262

Because wear rates are being measured over a rather short period of time, it is essential that the thruster operating parameters be stable for the duration of each test and that the thruster performance be reproducible with each iteration. After startup, the engine parameters generally stabilized after approximately 20–30 min of operation. The thruster appeared to perform similarly between subsequent tests, although over time the performance of the engine was noted to degrade with repeated exposures to atmosphere. Although the cathodes were reconditioned at the beginning of each test, it is suspected that the repeated exposure to the water vapor and oxygen in the air had an unfavorable effect on the cathode inserts, causing a small increase in discharge voltage and neutralizer keeper voltage with time.

Experimental Conditions and Results

A total of nine tests were conducted, each between 40 and 90 h in duration. The objectives of the first four erosion tests were to validate the SLA method as a viable wear diagnostic for ion thrusters and to establish the repeatability of the technique. These results are given in Table 5. Note that the location of the activated band is given as a function of the keeper outer radius, r_o.

The next five tests were aimed toward investigating the variation of wear rate due to changes in the keeper potential. The TH 8 throttle point was considered for this case because recent life test data suggest that a short between the keeper and the cathode may have accelerated the erosion rate at these operating conditions.[8] Two methods were used to bias the keeper positive with respect to cathode potential. First, an adjustable resistor was wired in parallel with the 1-kΩ resistor, which typically couples the anode to the keeper. In subsequent cases, the keeper was biased positive with a 0–30 V power supply. Results from tests conducted at four different keeper potentials are shown in Table 6. Data from two tests which were conducted with the purpose of establishing the erosion profile at this throttle point are shown in Table 7.

Discussion

Replication of the LDT Erosion Rates

The erosion rates measured by the SLA technique at TH 15 agree well with those calculated from the 8200-h keeper profile. A comparison of the LDT profile and the extrapolated wear after the same amount of time based on the SLA measurements is shown in Fig. 7. The gray regions denote the location of the activated bands. The profile shape from the LDT has been accurately reproduced, with the magnitude of the erosion rates measured to be 7–41% higher. After the tests were completed, noticeable texturing of the keeper surfaces was observed, as shown in Fig. 8.

To interpret the SLA results properly, note that the LDT profile represents the erosion rates integrated over the entire 8200-h test duration. As shown in Fig. 6, the discharge voltage of EMT2 varied between 23.1 and 24.9 V, the keeper voltage varied between 2.9

Table 5 TH 15 erosion rate test results

r/r_0	Test duration, h	8200-h erosion rate, μm/h	Measured erosion rate, μm/h	Mass loss rate, μg/h · mm^2	V_D, V	V_{CK}, V
0.341	70.9	0.0387	$0.0546^{+0.0022}_{-0.0028}$	$0.562^{+0.023}_{-0.028}$	23.86 ± 0.24	3.39 ± 0.10
0.540	80.4	0.0629	$0.0853^{+0.0033}_{-0.0053}$	$0.877^{+0.034}_{-0.054}$	24.07 ± 0.21	3.32 ± 0.17
0.735	74.8	0.0508	$0.0589^{+0.0024}_{-0.0026}$	$0.605^{+0.025}_{-0.027}$	23.92 ± 0.15	3.51 ± 0.10
0.735	51.8	0.0508	$0.0540^{+0.0023}_{-0.0023}$	$0.555^{+0.024}_{-0.024}$	24.15 ± 0.25	3.29 ± 0.33

Table 6 TH 8 erosion rates with different keeper potentials

r/r_0	Test duration, h	Measured erosion rate, μm/h	Mass loss rate, μg/hr · mm^2	V_D, V	V_{CK}, V
0.341	76.0	0.0311 ± 0.0014	0.320 ± 0.014	25.42 ± 0.22	7.88 ± 0.14
0.341	86.5	0.0349 ± 0.0014	0.359 ± 0.015	25.43 ± 0.13	6.04 ± 0.06
0.341	39.7	0.0401 ± 0.0017	0.412 ± 0.018	24.72 ± 0.19	2.48 ± 0.06
0.341	44.7	0.0538 ± 0.0023	0.553 ± 0.024	24.76 ± 0.24	0 (Shorted)

Table 7 TH 8 erosion profile test results

r/r_0	Test duration, h	Measured erosion rate, μm/h	Mass loss rate, μg/hr · mm^2	V_D, V	V_{CK}, V
0.341	39.7	0.0401 ± 0.0017	0.412 ± 0.018	24.72 ± 0.19	2.48 ± 0.06
0.540	44.5	0.0291 ± 0.0013	0.298 ± 0.014	24.69 ± 0.22	2.57 ± 0.10

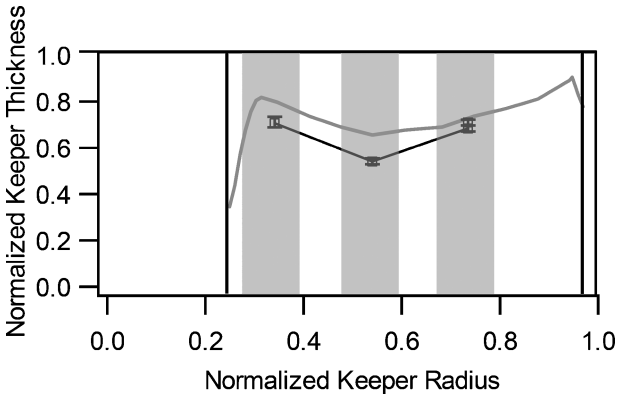

Fig. 7 Extrapolated erosion profile after 8200 h of operation at TH 15; LDT profile included for comparison: ——, 8200-h LDT profile and □, extrapolated profile from measured wear.

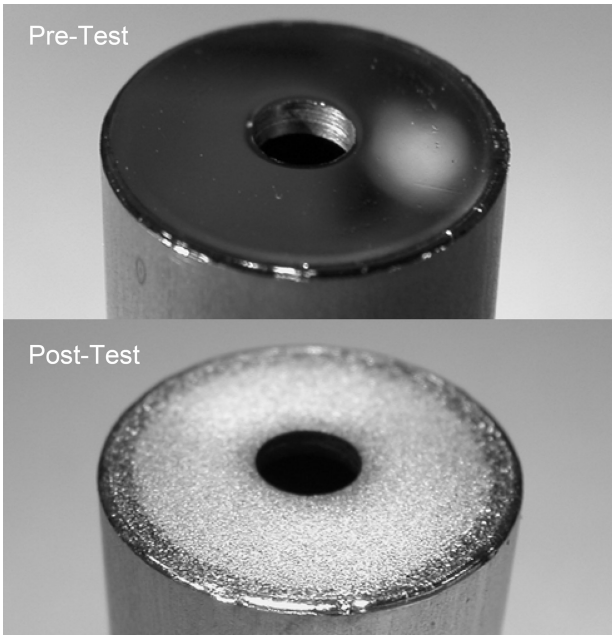

Fig. 8 Downstream keeper surface before and after 70 h of operation at TH 15.

and 5.3 V, and the keeper erosion rate also changed as a function of time. During the short duration of the SLA experiments, the performance of the NKO thruster was representative of the performance of NSTAR thrusters, but may not correspond to the averaged operating conditions of EMT2 during the LDT. This does not indicate that the wear rates predicted by SLA are unrealistic, but suggests that the SLA measurements are a snapshot of what the erosion rates in EMT2 were for a particular set of operating conditions. This is inherently true of all short-term wear diagnostics and is not a specific flaw associated with the SLA technique.

For the purpose of establishing margins on thruster component life, extensive life testing has been the technique of choice in the past. However, such wear testing has produced differences between tests, even when conditions are carefully controlled. For example, posttest analysis of the keeper from the 1000-h wear test indicates

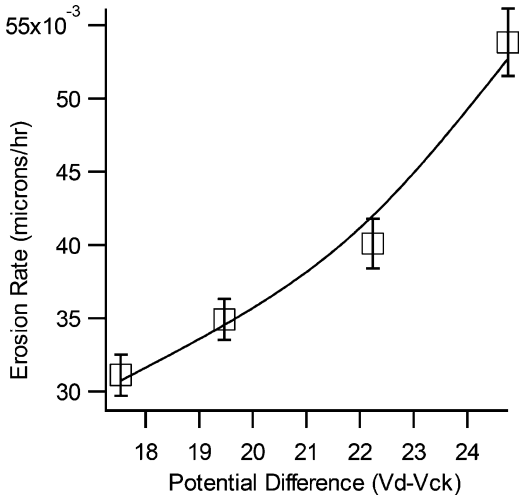

Fig. 9 Erosion rates as a function of keeper potential at the TH 8 throttle setting for the $r/r_o = 0.341$ position.

a maximum erosion rate of 0.070 μm/h, 11% higher than the maximum measured during the LDT.[4,6] Both tests included engineering model thrusters very similar to each other in construction, run under the same operating conditions. The authors suggest that if long-duration testing is not feasible, the SLA technique can provide results of comparable accuracy in a much shorter time frame. SLA may also be used to evaluate the sensitivity of erosion rates to different thruster operating parameters, another topic addressed by this investigation.

Repeatability

Although it was impractical to perform multiple tests for the same thruster operating conditions, it was desirable to examine the repeatability of results between the beginning of the test cycles to the end. As already mentioned, small changes in thruster performance were noticed after repeated exposures to atmospheric pressure between tests and could affect the erosion rate of the keeper. A test of the keeper activated at $r/r_o = 0.735$ for the TH 15 setting was conducted twice. The measured wear rates correspond closely with each other (to within 9%), and the calculated error bars for these points overlap.

Sensitivity of Erosion Rate to Keeper Potential

It was suspected that the keeper voltage substantially influenced the erosion rate, based on observations from the ELT. The energy of an ion that falls through the sheath between the discharge plasma and the keeper at a potential V_{CK} with respect to cathode is dependent on the voltage difference between the discharge plasma and the cathode keeper. It is reasonable to conclude that increasing the keeper voltage will reduce the ion energies at the keeper surface, thereby decreasing the erosion rate.

Four tests of the inner activated region were conducted at the TH 8 throttle point, with the keeper biased to different potentials. The results from this analysis are given in Table 6 and Fig. 9. When the keeper is shorted to the cathode, the erosion rate increases significantly and is comparable to the TH 15 nominal case at the same position. Increasing the keeper potential with respect to the cathode reduces the erosion rate monotonically. This was accomplished by decreasing the resistance between keeper and anode, allowing it to float at a higher potential with respect to the cathode. Applying a

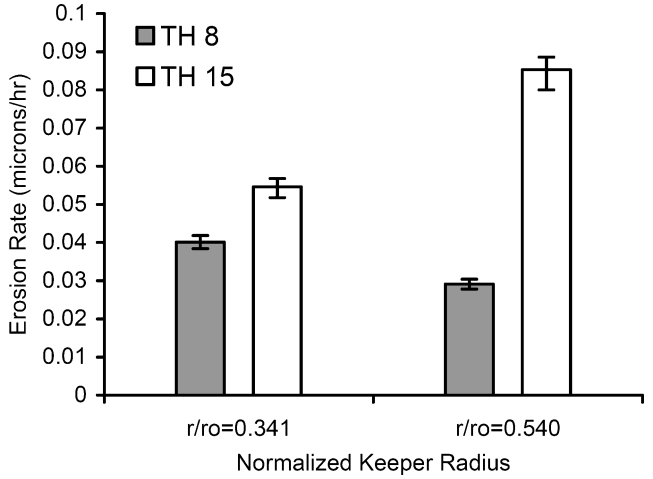

Fig. 10 Comparison of keeper downstream surface erosion rates for TH 8 and TH 15.

bias voltage of nearly 8 V decreases the erosion in the measured region to 0.0311 μm/h.

Variation of Erosion Rate with Throttle Level

Two tests at TH 8 were aimed at measuring the variation in the wear profile with distance from the keeper centerline. The data from these tests are shown in Table 7 and in Fig. 10. Erosion data with the NKO thruster at this operating point display two important attributes. First, the wear rates appear to be less overall at the lower throttle level than at TH 15. In addition, a different wear profile is shown with the most severe wear near the orifice.

The tests conducted in this investigation indicate that the measured wear at TH 8 is insufficient to have caused the rapid destruction of the keeper during the ELT. From the values obtained here, it is predicted that just over 50% of the orifice plate would have been eroded after 15,000 h of operation at the ELT throttle levels. However, ELT photographs display complete wear through at this position for the same amount of time. The wear rates along the orifice wall were not measured in this study and could be substantially greater than those on the downstream face.

The data obtained from the wear tests suggest possible courses of action for reducing the keeper erosion rate. Biasing the keeper with respect to cathode common could significantly enhance keeper life. This would a cause a slight decrease in total thruster efficiency resulting from the additional power required to operate the keeper bias supply. With a 7.50-V bias applied to the keeper, 0.372 A of current was used for a total power consumption of 2.79 W. Another course of action would be fabricating the keepers from materials with lower sputtering yields, such as carbon. Recent success in wear testing cathodes outfitted with carbon keepers suggest that this is a feasible option.[19]

Conclusions

The SLA method was validated in this investigation by reproducing the wear pattern observed in the 8200-h LDT at TH 15. The TH 8 erosion profile was found to differ significantly from the TH 15 profile. At TH 8, the wear is greatest near the orifice, as compared to the TH 15 condition, where the wear is largest near the middle of the profile. In addition, at the nominal TH 8 case, the erosion rates were significantly less than at TH 15.

Keeper potential appears to have a significant effect on the erosion rate. Four tests conducted at TH 8 indicate that the erosion rate increases significantly when the keeper is shorted to the cathode. Furthermore, biasing the keeper to a higher positive voltage can be used as a technique to combat erosion.

Wear tests on a laboratory model thruster produced erosion data for eight different operating conditions, each after only 40–90 h of operation. Evaluation of this number of conditions using conventional long-duration testing would have required thousands of hours of operation. Tests similar to these could be applied in future propulsion projects to measure accurately the erosion rates of cathode and grid components. Such measurements could be used to identify potential life-limiting phenomena, validate models of wear processes, and to help qualify engines for the required service life.

Acknowledgments

Robert Kolasinski acknowledges the National Science Foundation for funding his graduate research while at the California Institute of Technology. The research described in this paper was conducted in part at the Jet Propulsion Laboratory, California Institute of Technology, and was sponsored by NASA. The authors gratefully acknowledge Kenneth Oxorn of ANS Technologies for his valuable advice in choosing the activation parameters and for performing the actual activations. In addition, the authors also express their appreciation to Allison Owens at the Jet Propulsion Laboratory, who was responsible for fabricating the NKO thruster.

References

[1]Polk, J. E., Goebel, D., Brophy, J. R., Beatty, J., Monheiser, J., Giles, D., Hobson, D., Wilson, F., Christensen, J., De Pano, M., Hart, S., Ohlinger, W., Hill, D. N., Williams, J., Wilbur, P., Laufer, D. M., and Farnell, C., "An Overview of the Nuclear Electric Xenon Ion System (NEXIS) Program," AIAA Paper 2003-4713, July 2003.

[2]Brophy, J. R., Polk, J. E., and Rawlin, V. K., "Ion Engine Service Life Validation by Analysis and Testing," AIAA Paper 96-2715, July 1996.

[3]Patterson, M. J., Rawlin, V. K., Sovey, J. S., Kussmaul, M. J., and Parkes, J., "2.3 kW Ion Thruster Wear Test," AIAA Paper 95-2516, July 1995.

[4]Polk, J. E., Patterson, M. J., Brophy, J. R., Rawlin, V. K., Sovey, J. S., Myers, R. M., Blandino, J. J., Goodfellow, K. D., and Garner, C. E., "A 1000 Hour Wear Test of the NASA NSTAR Ion Thruster," AIAA Paper 96-2784, July 1996.

[5]Polk, J. E., Anderson, J. R., Brophy, J. R., Rawlin, V. K., Patterson, M. J., Sovey, J., and Hamley, J., "An Overview of the Results from an 8200 Hour Wear Test of the NSTAR Ion Thruster," AIAA Paper 99-2446, June 1999.

[6]Domonkos, M. T., Foster, J. E., and Patterson, M. J., "Investigation of Keeper Erosion in the NSTAR Ion Thruster," International Electric Propulsion Conf., IEPC Paper 01-308, Oct. 2001.

[7]Williams, G. J., Smith, T. B., and Gallimore, A. D., "30 cm Ion Thruster Discharge Cathode Erosion," International Electric Propulsion Conf., IEPC Paper 01-306, Oct. 2001.

[8]Sengupta, A., Brophy, J. R., and Goodfellow, K. D., "Status of the Extended Life Test of the Deep Space 1 Flight Spare Ion Engine after 30,352 Hours of Operation," AIAA Paper 2003-4558, July 2003.

[9]Kosako, T., and Nishimura, K., "The Thin Layer Activation Technique Applied to the On-Line Iron Wear Measurement of an Engine Cam Nose," *Nuclear Instruments and Methods in Physics Research B*, Vol. 56-7, May 1991, pp. 900–903.

[10]"Thin Layer Activation Method and its Application in Industry," International Atomic Energy Agency, Rept. IAEA TECDOC-924, Vienna, Austria, Jan. 1997.

[11]Ditrói, F., and Mahunka, I., "Thin Layer Activation of Non-Metallic Materials by Using Nuclear Implantation," *Nuclear Instruments and Methods in Physics Research B*., Vol. 113, June 1996, pp. 415–419.

[12]Marks, L. M., Clark, K. E., von Jaskowsky, W., and Jahn, R. G., "MPD Thruster Erosion Measurement," AIAA Paper 82-1884, Nov. 1982.

[13]Polk, J. E., "Mechanisms of Cathode Erosion in Plasma Thrusters," Ph.D. Dissertation, Dept. of Mechanical and Aerospace Engineering, Princeton Univ., Princeton, NJ, Nov. 1997.

[14]Wallace, G., "Calculation of Depth Profile for Thin Layer Activation," International Atomic Energy Agency, Client Rept. 62891H 11, Vienna, Austria, March 1999.

[15]Ziegler, J. E., Biersack, J. P., and Littmark, U., *The Stopping and Range of Ions in Solids*, Vol. 1, Pergamon, Oxford, 1985.

[16]Schonfeld, E., Kibbey, A. H., and Davis, W., Jr., "Determination of Nuclide Concentrations in Solutions Containing Low Levels of Radioactivity by Least-Squares Resolution of the Gamma-Ray Spectrum," *Nuclear Instruments and Methods*, Vol. 45, Nov. 1966, pp. 1–21.

[17]Unik, J. P., and Rasmussen, J. O., "Decay Schemes of the Isomers of Tc^{95} and Tc^{97}," *Physical Review*, Vol. 115, No. 6, 1959, pp. 1687–1692.

[18]Schilling, W., and Ullmaier, H., "Physics of Radiation Damage in Metals," *Materials Science and Technology: A Comprehensive Treatment*, Vol. 10 B, VCH Publishers, New York, 1994, pp. 179–241.

[19]Hayakawa, Y., Kitamura, S., Miyazaki, K., Yoshida, H., Akai, K., and Kajiwara, K., "Wear Test of a Hollow Cathode for 35-cm Xenon Ion Thrusters," AIAA Paper 2002-4100, July 2002.